

Temporal pulse manipulation and consequences for ultrafast laser processing of materials

Razvan Stoian¹

Alexandre Mermillod-Blondin¹

Sebastian W. Winkler²

Arkadi Rosenfeld

Ingolf V. Hertel³

Max-Born Institut für Nichtlineare Optik und
Kurzeitspektroskopie

Max Born Str. 2a

D-12489 Berlin, Germany

E-mail: stoian@mbi-berlin.de

Maria Spyridaki⁴

Emmanuel Koudoumas⁵

Panos Tzanetakos⁴

Costas Fotakis⁴

Institute of Electronic Structure and
Laser

Foundation for Research and Technology-
Hellas

P.O. Box 1527

71110 Heraklion, Greece

Igor M. Burakov

Nadezhda M. Bulgakova

Institute of Thermophysics SB RAS

1 Acad. Lavrentyev Avenue

630090 Novosibirsk, Russia

Abstract. Following advances in ultrafast laser technology as a reliable tool for material probing and processing, we discuss various options for control and optimization. The possibility to tailor the temporal shape of ultrashort laser pulses enables extended opportunities for material processing. The concept of optimizing laser interactions is based on the possibility to regulate the energy delivery so that control of laser-induced phenomena can be achieved and quality structures can be realized. An experimental demonstration of the possibility to design excitation sequences tailored with respect to the material response is described, laying the groundwork for adaptive optimization in materials structuring. We show that under particular irradiation conditions involving modulated excitation, the energy flow can be controlled and the material response can be guided to improve processing results. This is particularly important for processing brittle materials. Further examples are given to illuminate the possibility to optimize the kinetic properties of ions emitted from laser-irradiated semiconductors, using excitation sequences synchronized with the solid-to-liquid transformation time. Versatile sub-kilo-electron-volt ion beams are obtained, exploiting transitions to supercritical fluid states with minimal energetic expenses. Temporally selective irradiation can thus open up efficient thermodynamic paths, unfolding interesting perspectives for "intelligent," feedback-assisted processing of materials.
© 2005 Society of Photo-Optical Instrumentation Engineers. [DOI: 10.1117/1.1915467]

Subject terms: ultrafast laser ablation; pulse shaping; adaptive optimization; material processing.

Paper 040507 received Jul. 27, 2004; revised manuscript received Oct. 12, 2004; accepted for publication Nov. 18, 2004; published online May 13, 2005.

1 Introduction

Advances in ultrafast pulsed laser technologies have made it possible to investigate physical processes on the shortest time scale and to structure materials with optical resolution.¹⁻⁵ The potential of ultrashort laser pulses for material processing is based primarily on the possibility to localize energy deposition and to reduce residual damage by minimizing thermal artefacts.¹⁻⁹ Thus, important demands for miniaturization and integration in micro- and nanofabrication techniques can be achieved. As mentioned, the enhanced capabilities for reduced-scale processing rely on strong nonlinear, nonthermally driven interactions, reduced heat effects, and, more recently, the unique possibility of pulse-adaptive manipulation.¹⁰ The technological development of rapid optical modulation devices¹¹ and the implementation of robust adaptive numerical procedures for optimization of predefined experimental outputs have enabled the generation of complex electromagnetic waveforms in the IR and visible spectral ranges and have provided an efficient instrument to control and manipulate the

interaction between light and matter. The capability to tailor ultrashort laser pulses to desired temporal shapes exploits the large spectral bandwidth of the laser pulse and the possibility to have complete control over the spectral characteristics of the electrical field. Temporal pulse shaping by complex Fourier synthesis of spectral components is an effective technique able to control and optimize optical transitions in a variety of physical and chemical systems using coherent light, and to route particular processes in prespecified directions. Optimal control experiments have addressed several types of physical situations, including selective breaking of chemical bonds, manipulation of electron transfer in biological complexes, design of particular molecular vibrations, enhancement of radiative high harmonics, or creation of ultrafast semiconductor switches.¹²⁻¹⁹ Particularly for complicated systems, whenever the optimal optical waveform to assist a specific transition is not straightforward, adaptive optimization procedures may deliver the most effective way to drive the systems in prespecified states. The extreme irradiation conditions created by ultrashort laser pulses have also enabled generating previously unexplored properties of materials around thermodynamical critical points. Ultrafast laser-driven phase transitions and exotic metastable states are some of the observations that point toward the potential of obtaining singular laser machining technologies suitable for a broad range of applications. These novel techniques are conceived to generate new matter properties and phases

¹Also at Laboratoire TSI (UMR 5516 CNRS), Université Jean Monnet, Saint Etienne, France.

²Present address: University of Georgia, Athens, Georgia, USA.

³Also at Freie Universität Berlin, Fachbereich Physik, Berlin, Germany.

⁴Also at University of Crete, Physics Department, Heraklion, Greece.

⁵Also at Technological Educational Institute of Crete, Electrical Engineering Department, Heraklion, Greece.

0091-3286/2005/\$22.00 © 2005 SPIE

based on synergies with the material intrinsic response, thus unfolding new perspectives for “intelligent,” feedback-assisted processing of materials.

Therefore, in addition to the substantial scientific interest, the concept of adaptive optimization has significant practical implications, stimulating new ideas and potential in advanced laser material processing. The potential spectrum of applications ranges from quality structuring of materials for increased functionality to integration in analytical methods sensitive to particle emission or to controlling ion beams for implantation purposes. To improve processing results, the efforts followed two main technological paths: materials with engineered characteristics for optimal intrinsic energy coupling (e.g., photosensitivity enhancement) and laser radiation tailored with respect to the transient material properties. In the latter case, while the laser energy delivery rate will be adaptively adjusted to the best coupling conditions, the materials themselves will play an active role in the structuring process.

In the specific aspect of improving and controlling the characteristics (flux, energy, angular distribution) of the ion beams induced by laser ablation for micro- and optoelectronic applications (e.g., quantum dot formation at the Si/SiO₂ interface using shallow implantation), temporal pulse shaping is particularly promising, with the potential to compensate the current deficit in the properties of the sub-kilo-electron-volt high-flux ion beams delivered by presently available commercial techniques. Therefore, we propose a procedure based on evolutionary algorithms using phase modulation and, subsequently, temporal pulse tailoring as a functional degree of freedom to improve the kinetic characteristics of a Si ion beam emitted from laser-irradiated silicon targets at moderate fluences.²⁰ We demonstrate that by optimizing the energy delivery rate impinging on the silicon target we can take advantage of a succession of phase transformations, drive the system in specific thermodynamic states, and obtain controllable low-kinetic-energy and high-flux ion beams for practical purposes, among them ion implantation. The various characteristics of the ion beams such as kinetic energy, ionization degree, and directionality can influence ion implantation results since they can affect the penetration profiles of the impurities. Essentially, in optimization experiments the measured output is fed back into an iterative learning loop until a particular excitation sequence properly adapted to the experimental conditions is determined, without any initial information on the physical parameters. Since no prior knowledge of the physical aspects of the problem is required, evolutionary algorithms can be applied to find optimal solutions for a wide class of problems, from coherent control of electronic and nuclear degrees of freedom in complex physical, chemical, and biological systems to process optimization in practical applications. Moreover, as anticipated before, a demonstration of designing material-removal characteristics from laser-irradiated materials is appealing for a broader range of scientific and technological applications. We will address in this review aspects of recent experimental progress concerning material behavior under modulated laser excitation with relevance to laser ablation and application fields.

2 Experiment

For most of the experiments, unless otherwise mentioned, dielectric [fused silica (a-SiO₂), sapphire (Al₂O₃)] and semiconductor (Si) samples were irradiated under vacuum conditions (10⁻⁵ mbar) with 170-fs pulses from an 800-nm Ti:sapphire oscillator-amplifier laser system delivering 0.6 mJ energy per pulse at a nominal repetition rate of 100 Hz. The laser system incorporates a closed-loop programmable pulse-shaping apparatus and additional ion detection devices. For ion recording, the *p*-polarized laser beam was focused onto the sample surface at 24 deg incidence down to a spot of approximately 950 μm². An electromechanical shutter was used to control the irradiation dose, scaling the repetition rate down to 1 Hz, and releasing a controllable number of pulses. The energy in the laser pulse was varied using neutral filters and a half-wave plate in combination with a thin film polarizer.

Temporal pulse tailoring¹¹ was realized by dynamically altering the spectral phase of an incident bandwidth-limited laser pulse, which is spatially dispersed and reformed in a zero-dispersion unit that includes a 640-pixel liquid crystal (LC) modulator (Jenoptik) in the Fourier plane. The use of LC modulators in spatially dispersed beams enables phase/amplitude modulation (by controlled retardation and attenuation at each pixel position in the frequency space), introducing different optical paths to the spatially separated spectral components and, in turn, tailoring the pulses to the desired temporal shapes. Our setup was used in the phase-only modulation scheme, thus keeping constant the energy in the pulse, which was then delivered at different rates. The optical modulator was inserted after the oscillator, the amplifier being seeded with the phase-modulated beam. Therefore, small energy variations determined by the spectral phase modulation are minimized and the beam is regenerated spatially and energetically. The temporal profile of the modulated sequence was measured by second-order cross-correlation with a nonmodulated pulse deflected from the oscillator prior to phase modulation and seeded in the amplifier 500 ps after the modulated pulse.

Positively charged ions were detected by a linear time-of-flight^{21,22} (TOF) mass spectrometer in a Wiley-McLaren configuration, with the detection axis normal to the sample surface. The emitted ions were allowed to drift for 65 mm in a field-free region, then extracted into the mass spectrometer with a pulsed electric field from a restricted region of 9 mm, and detected with a microsphere plate (MSP) situated at a distance of 289 mm from the target. The pulsed voltage applied on the extraction grids at different delay times with respect to the laser pulse enables the construction of the mass-resolved velocity distribution at the position of the extraction region. The variable extraction-field delay samples the expanding ablation plume temporally and the ion signal recorded for a given extraction time corresponds to a well-specified velocity of the ions. The TOF mass spectrometer has the additional possibility to be used without pulsed extraction, consequently suppressing the mass resolution, but enabling the measurement of the flight time of the emitted charge from the target to the detector. Without going further into details, we note briefly that, using postionization sources and repelling voltages for the primary ions, the same experimental

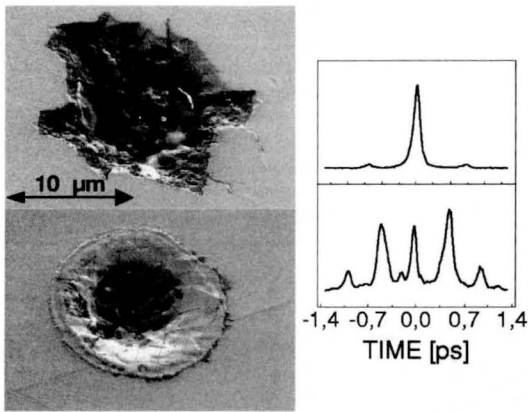


Fig. 1 Laser-induced structures on CaF_2 with single-pulse (upper part) and triple-pulse sequences (bottom part) with 0.5-ps separation. The results show improvements for the structures realized by temporally modulated excitation. The number of pulses used to form the structures was $N=5$ and the laser fluence was 7 J/cm^2 and, respectively, 12 J/cm^2 .

setup can be used to monitor the neutral emission from the irradiated samples.

Ex situ examinations of the irradiated region were performed using optical (OM), atomic force (AFM), and scanning electron microscopy (SEM).

3 Results and Discussion

The possibility to synchronize the laser radiation with the material response and to realize synergies between radiation and matter has some interesting consequences for material processing by assigning an active role to material intrinsic and transient properties. A temporally shaped laser

pulse can induce a modulated electronic excitation with the possibility to achieve a certain degree of control for the subsequent electronically induced structural transformations. Brittle dielectrics irradiated with temporally shaped pulses¹⁰ above the damage threshold have indicated the possibility to improve the structuring process and to eliminate fracturing based on a fast laser-induced brittle-to-ductile transition.²³ An example of using suitable multipulse irradiation with terahertz repetition rates (subpicosecond separation) on brittle fluoride materials is presented in Fig. 1, resulting in improved, low-stress structures as compared to single-pulse processing. The interaction is regulated by the fast trapping of the laser-generated free electrons^{24–27} that cause lattice deformations and transient atomic displacements, softening the irradiated surface on a subpicosecond time scale. In this way, the initial pulses in the excitation sequence prepare the surface for optimal coupling of the subsequent pulses. Moreover, for dielectric materials with strong electron-phonon interactions (e.g., amorphous SiO_2), excited with multipulse sequences with picosecond separation, the irradiated spot shows a spatially modulated depth profile,²⁸ the consequence of modulated coupling properties as depicted in Fig. 2(a). On the other hand, a single short pulse or short multipulse separation (below 0.3 ps) results in smooth hemispherical profiles.²⁸ The modulated absorption is determined dominantly by the fast transient buildup of self-trapped excitonic states in fused silica. Theoretical modeling based on a 2-D extension of the energy transport model developed by Bulgakova et al.,²⁹ taking into account free-electron generation under the laser action as well as energetic losses due to electron trapping, indicates the establishment of a nonuniform temperature profile in the sample after sequential energy delivery [Fig. 2(b)] on a

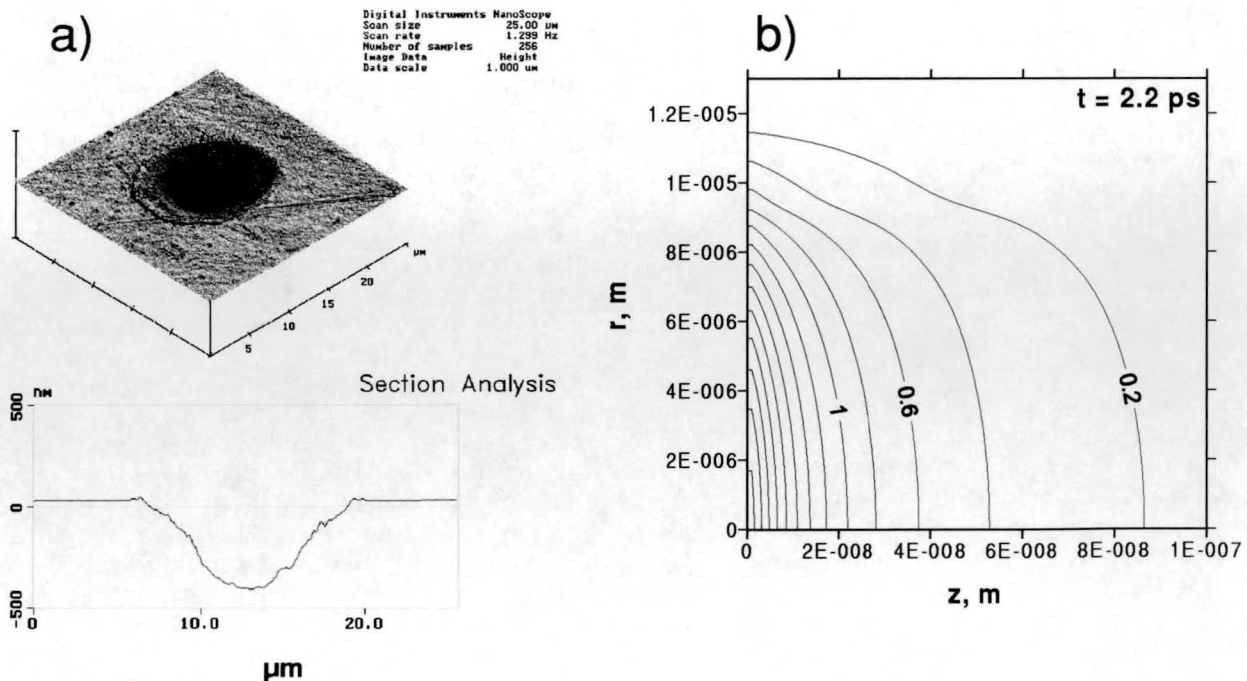


Fig. 2 (a) Single shot structures made on a- SiO_2 surfaces with triple pulses separated by 1 ps at 14 J/cm^2 , where the temporal modulation of the pulse train leads to a depth modulation of the spatial profile, and (b) 2-D temperature profile in the a- SiO_2 sample at the end of the excitation sequence.

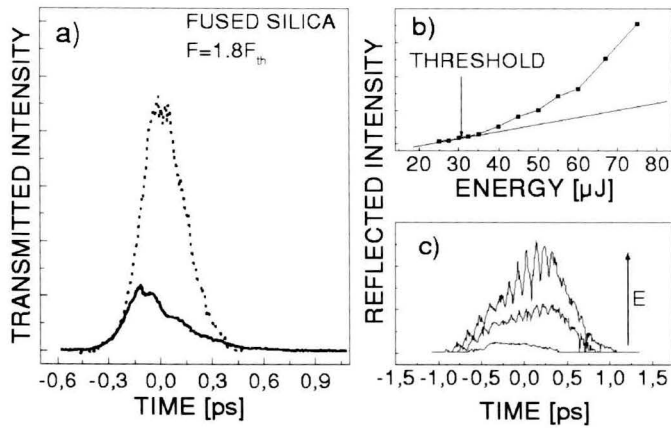


Fig. 3 (a) Temporal profile of the laser pulse with intensity above the damage threshold, before (dotted line) and after (solid line) passing a 200- μm -thick fused silica slab. The profiles are obtained by cross-correlation with a reference Fourier-limited pulse. The tail of the laser pulse is absorbed in the laser-induced electron plasma. (b) Reflected part of the laser pulse at different irradiation energies and (c) temporal profile of the reflected part of a 1-ps-long laser pulse on the self-induced electron plasma at the air-dielectric interface at different input energies below and above the damage threshold.

picosecond time scale. At the same time, the equipotential energy surfaces, describing the energy stored in defect states and, subsequently, in lattice deformations, have a similar (not shown) spatial modulation.

Monitoring laser-induced transient optical properties of transparent materials and the effects of the self-action of the laser pulse enables access to the primary excitation processes during irradiation and may be developed into an efficient feedback instrument for the interaction process. The leading edge of the laser pulse, at above damage fluences, creates a dense electronic population in the conduction band based on a multiphoton seeded electron multiplication process. The transition to the critical density generates collective electron oscillations at the laser frequency and automatically transforms the material into a strong absorber/reflector for the trailing edge of the pulse. Figure 3 shows examples displaying the self-action of the laser pulse creating the free-electron gas on the transmitted, respectively, reflected radiation, at different input energies in the vicinity of the damage threshold at normal incidence. Different details of the interaction process can be extracted from the temporal profile of the transmitted short Gaussian pulse (170 fs) through the interaction area. Figure 3(a) indicates the corresponding temporal envelope of an initially Fourier-transformed laser pulse after passing a 200- μm dielectric slab (fused silica) at input fluences above the damage threshold. The temporal profile is obtained from a second-order background-free cross-correlation with an independent bandwidth-limited 170-fs laser pulse. For an unambiguous discrimination between different absorption processes, it is imperative that the nonlinear propagation effects in the bulk that affect additionally the spatial and the temporal profile can be precisely accounted for. Scanning the input energy density below and above the material damage threshold and measuring the amount of reflected light, a sudden increase is observable at the transition to a plasma mirror state with supercritical carrier densities [Fig. 3(b)].

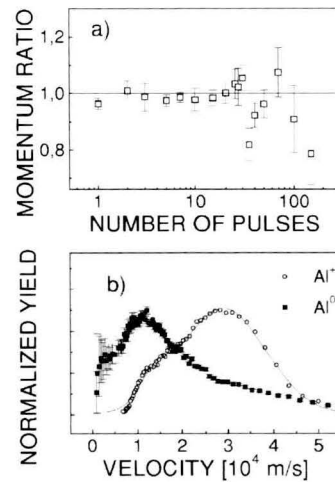


Fig. 4 (a) Momentum ratio for different ionic species (O^+ , respectively, Al^+) emitted from laser-irradiated sapphire (Al_2O_3) samples at fluences slightly above the damage threshold and (b) velocity distributions of ionic and neutral aluminum atoms removed from sapphire samples in similar conditions as in (a).

Similar observations can be made by monitoring the temporal profile of the self-reflected beam. The increased asymmetry of the profile at above threshold fluences defines the temporal onset of the plasma mirror [Fig. 3(c)]. This specific type of investigation enables a precise assessment of the balance between multiphoton and collisional excitation in excited materials. Moreover, it enables subsequent balancing of the two complementary processes and provides access to the properties of the laser-induced electron plasmas under variable irradiation conditions.

Previous time-resolved experiments on laser-induced ion emission from different classes of materials^{30,31} have indicated significant differences between dielectrics, semiconductors, and metals. Based on energy and momentum considerations, the results have clearly demonstrated the presence of a Coulomb-exploded component in the distribution of ions removed from dielectric surfaces. This is a consequence of strong photoelectron emission and of poor carrier transport in the irradiated region that allows significant charging of the surface and impulsive repulsion of the ionic layers. The impulsive material removal results in emission of ions characterized by the same momenta [Fig. 4(a)], which is a signature of a sudden, electrostatically driven process. Figure 4(b) shows the ionic and neutral velocity distribution for Al atoms emitted from sapphire samples and reflects the impulsive nature of the acceleration mechanisms for the ionic component. At the same time, the *in situ* time-resolved measurements^{30,31} have indicated the absence of the electrostatic breakup of the surface for conducting and semiconducting materials in the vicinity of the ablation threshold, and a significant increase in the efficiency of ion emission from silicon on a picosecond time scale, in very good agreement with time-resolved x-ray diffraction detection of the thermal response of the Si lattice.^{32,33}

Semiconductor excitation by ultrafast laser irradiation^{34–39} at fluences around the damage threshold has revealed the appearance of a high-reflectivity, almost metal-like phase on the development of a dense electron-hole

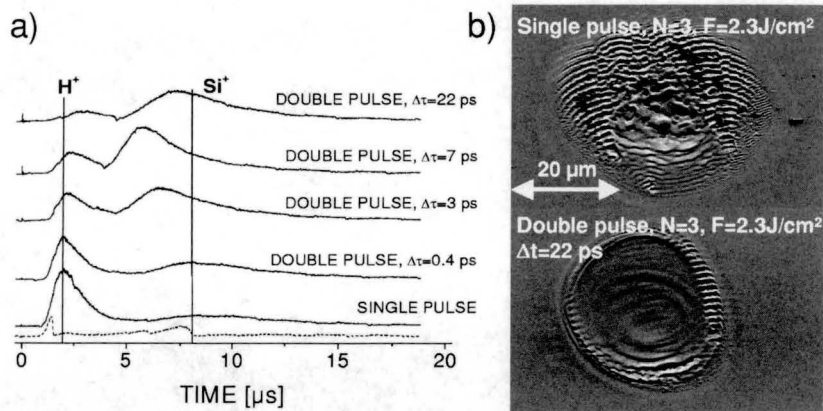


Fig. 5 (a) Non-mass-resolved TOF ion spectra from silicon targets under ultrafast laser irradiation with single and double pulses with increasing separation times at 0.9 J/cm^2 total incident fluence. To demonstrate the species content of the features, a short-range retarding positive voltage of 200 V was applied in front of the charge detector (dotted line). (b) SEM images of the laser-induced structures generated after three successive irradiation sequences of single and double, 22-ps-separated pulses of 2.3 J/cm^2 total fluence on the same spot. While the single-peak irradiation generates significant melt residuals, suggesting strong thermal and hydrodynamic activity, double-pulse irradiation produces cleaner structures by efficiently coupling the second pulse into the previously induced liquid region.

plasma with the optical response of a free-electron gas. When an intense light beam carrying photons of sufficient energy to overcome the bandgap illuminates the semiconductor, free carriers are generated via one- and two-photon interband absorption followed by further free-electron heating. If a specific threshold is surpassed and a significant number of electrons is pumped in the conduction band, the strong electronic excitation is almost immediately followed by premature bond softening, lattice destabilization, and the appearance of nonthermal phase transitions on a subpicosecond time scale. The ultrafast lattice disordering induced primarily by electronic excitation in antibonding states precedes the thermal phase transformations. For lower energy inputs, screened nonradiative recombination, delayed carrier-lattice thermalization, and phonon equilibration together with thermal transport limited by the velocity of sound will force the characteristic time for the thermal melting at a timescale of a few picoseconds. Material removal proceeds via the hydrodynamic expansion of the excited matter.

Based on the preceding characteristics, directional ion emission from laser-irradiated silicon samples is an interesting candidate for pulse tailoring experiments at a picosecond timescale due to the benefit of a succession of fast electronic and structural changes triggered by the laser radiation. For the initial experiments, the Si samples were irradiated with double ultrafast (180-fs) pulses with equal intensities and separation distances that varied between few hundred femtoseconds and 22 ps. Figure 5(a) displays the TOF spectra of the detected charge without mass resolution except the indication given by the characteristic drift of species with different masses. In this case, no intermediate electric fields influenced the flight of the particles from the sample to the MSP charge detector. The traces were recorded for single-pulse interaction and four cases of double-pulse sequences temporally separated by 0.4, 3, 7, and 22 ps, but with identical energy content. The silicon samples were repeatedly exposed to six excitation sequences per site at a 2-Hz repetition rate and 0.9 J/cm^2 total

incident energy density. A double-peak distribution is present, with the first peak centered at around $2\text{-}\mu\text{s}$ arrival time and containing dominantly positive hydrogen ions with energies below 300 eV. At this moderate fluence, we did not observe energetic (in the keV range) particles, as claimed in previous reports.⁴⁰ The hydrogen yield is a consequence of the laser-activated hydrogen emission following water dissociative adsorption on the silicon sample. The composition of the two peaks was verified using a positive retarding field in front of the MSP detector having the function of a high-pass energy filter. A 200-V retarding field almost entirely removes the first peak. The characteristic cut-off times of the barrier in the second peak indicate the presence of Si ions, mainly single ionized for single-pulse irradiation. Under our experimental conditions, double-pulse irradiation with picosecond separation favors, to a certain extent, the appearance of multiple ionized species and produces an evident energy gain for the single ionized silicon atoms as compared to the single-pulse irradiation. The position of the second peak depends strongly on the laser energy delivery rate showing a downshift of almost $3 \mu\text{s}$ as we increase the time separation of the two pulses, a tendency opposed to the H^+ peak behavior. The obvious dynamics of this feature suggest the possibility of using better-designed optical waveforms to control the interaction.

The improved efficiency of ion emission with increasing pulse separation on the picosecond scale may suggest a gas-phase interaction, although the separation times in the double-pulse sequence are too short to allow substantial gas-phase expansion and delayed ionization of neutrals emitted by the second pulse. Moreover, the leading pulse alone does not have enough energy to induce significant material removal. Concomitantly, the morphology of the damage [Fig. 5(b)] suggests a direct coupling to the thermally affected solid.⁴¹ For separation distances longer than 3 ps, the following scenario can be considered. The excitation induced by the first pulse degenerates into a significant

melting zone with altered optical properties, characteristic to the hot, liquid silicon. The second pulse couples very efficiently to the liquid layer, leads to total vaporization of the melted region, and leaves behind a featureless structure without the residual cast [Fig. 5(b)]. In contrast, single-pulse irradiation produces significant thermal and hydrodynamic effects in the residual melt that affect the quality of the structure. An optimal separation between the pulses corresponds to the formation of a liquid layer with a thickness similar to the optical penetration depth and leads to the formation of smooth structures on the surface.

In a second round of experiments, we applied adaptive numerical schemes to optimize the kinetic properties of the Si ion beam.⁴² The pulse was dynamically adapted to optimize the experimental result in a closed, self-learning feedback loop.⁴³

From a general point of view, one can say that the selectivity in generating high carrier densities in semiconducting materials is reduced⁴⁴ since all the accessed states in the conduction band will contribute to the current flow. In this case, the selection will rely on the more favorable energetic pathway with respect to the final lattice temperature. For irradiation doses specific to the ablation regime, rapid electronic dephasing in overcritically excited silicon severely reduces the possibility of triggering coherent processes, especially when the final state belongs to the continuum. As opposed to quantum control strategies where one tries to obtain electromagnetic fields designed to drive the system in final target quantum states, we build here on the temporal succession of different types of phase transformation, adapting the laser energy delivery rate to a succession of structural changes that give access to both ultrafast, nonthermally driven interactions, as well as to classical thermal domains.

The amplitude of the ion signal within a chosen velocity range ($\sim 4.2 \times 10^4$ m/s) serves as feedback for the optimization loop. To select the specific velocity, the pulsed extraction delay time in the TOF setup was set to the corresponding fixed value. The use of velocity windows adds flexibility to the process of manipulating the ion beam and enables us to control different portions of the velocity distribution. It is expected that the choice of different velocity windows may affect the result of the optimization, since the ejected particles may correspond to different times, mechanisms, and regions of emission, determined by the energy stored in different subsurface layers. The highest efficiency in manipulating the ion beam is reached in the high-velocity range.

The optimization of the ion yield is performed using a self-learning evolutionary strategy that produces suitable phase masks and programmable manipulation of the time-domain laser pulse envelopes. The procedure starts from a complex of arbitrary or reasonable-guess functions for the initial phase patterns applied on the optical modulator, which then evolves through genetic propagators. Evolution operators such as crossover and mutation are applied to search the solution space efficiently. The results are ranked according to their fitness (the measured value of the quantity to be optimized, in our case the magnitude of the velocity-resolved ion yield), and the algorithm will suggest an improved collection of solutions, searching the multidimensional space in a way similar to biological evolution.

For our specific purpose, the optimization sequence begins with a partially random population of 25 discrete phase masks on the modulator, including also the single, Fourier-transformed pulse and sometimes solutions obtained by previous runs of the algorithm. Assessing the signal, the algorithm tries out phase patterns originating from the adaptive combination of previous phase populations and iteratively proposes solutions based on the "survival of the fittest" selection procedure until convergence is achieved. The speed of convergence can be controlled by the input parameters of the algorithm (e.g., adaptive mutation step, size of population, number of parents used for crossover). Due to the limited size of the sample, we preferred to work with a relatively high and smooth convergence speed. No constraints related to the phase smoothness across the optical modulator were applied. Details concerning global optimization methods describing suitable use of crossover and mutation selection rules to ensure efficient exchange of information, genetic diversity, and to prevent trapping in local minima can be found elsewhere.⁴³

The value of the measured ion yield for an appropriate phase mask indicates the pulse capability to perform the specified task. The signal enhancement via the trial-and-error procedure instructs the laser iteratively to push the system in a thermodynamic state where the highest temperatures can be achieved with minimal energetic losses, based on the measured success of previous pulses. Minimal information about the physical insight is required at the beginning, but the optimal pulse includes the acquired knowledge concerning the mechanisms of control. The limitations of the shaping device are given by the upper boundary of the shaping temporal window, which relates to the spectral resolution of the zero-dispersion unit. In our case, this was limited to 22 ps.

The result of the optimization run offers the means to understand and control the laser-induced structural modifications that transiently change the coupling properties of the incoming radiation. Improvements are achieved even when the topology of the solution space is very complex and the selectivity of the excitation is reduced, allowing for a large class of solutions for a defined target. The algorithm provides similar solutions as long as sufficient energy is provided. At low energies, close to the ion detection threshold, the algorithm returns a single short pulse. The results are physically meaningful since only the highest intensity provided is able to take advantage of higher order absorption to generate an electron density sufficient to trigger the subsequent series of thermodynamic processes. The evolution of the system during the global optimization run is presented in Fig. 6(a) for a spatially averaged fluence of 0.8 J/cm^2 , approximately four to five times above the observed damage threshold. The task to maximize the ion yield with the velocity of 4.2×10^4 m/s [Fig. 6(b)] with an increase of almost 10 times as compared to the yield produced by single pulses delivers as the optimal intensity envelope a sequence of two pulses; a fast, short peak followed by a long pulse after approximately 8 ps [Fig. 6(c)]. Measuring the relative energy balance between the two pulses, one finds as an essential feature that the energy content of the first pulse (approximately 20 to 25% of the total energy) always levels out at the thermal solid-to-liquid phase transition threshold, realizing the minimal energetic require-

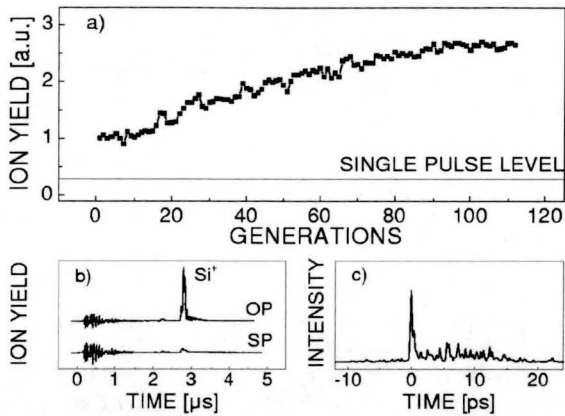


Fig. 6 (a) Evolution of the Si^+ ion yield during the adaptive optimization run, where a several-fold increase is obtained for the ion yield with a velocity of 4.2×10^4 m/s at a fluence of 0.8 J/cm^2 ; (b) TOF mass-resolved Si^+ trace corresponding to the single pulse and the optimal pulse, respectively; and (c) intensity envelope of the optimal pulse.

ments to induce the structural change. By judiciously redistributing the laser energy, the excitation sequence prepares the irradiated region for the most effective coupling conditions. A higher energy of the initial pulse will force the nonthermal disordering, losses will increase due to the higher reflectivity, and less energy will be available to heat the residual melt. Once the liquid phase is nucleated over a depth of a few nanometers, the second pulse couples, always in a molten, metallic-like phase dominated by one-photon intraband transitions. The absorption coefficient is dramatically enhanced⁴⁵ up to $\alpha_{\text{liquid}} = 10^8 \text{ m}^{-1}$ and most of the energy of the second pulse is deposited within the first nanometers, leading to a significant increase in the energy density confined in the liquid layer. The match between the thickness of the liquid layer and the absorption length of the pulse also has extended consequences for material structuring, because a sharper temperature gradient at the liquid-solid interface is equivalent to restricting the interaction to the molten region. Therefore, the ion flow is manipulated by the thermally induced transition to the molten phase and further energy deposition in the overheated liquid layer. Moreover, due to the somehow poorer electrical properties of liquid silicon as compared to a typical metal (electrical resistivity is $75 \mu\Omega \text{ cm}$ in the liquid phase, implying a low electron mobility of $\sim 1 \text{ cm}^2/\text{Vs}$, while thermal conductivity drops two orders of magnitude), carrier transport is inhibited and the energy has reduced means to diffuse away from the interaction region, establishing conditions to reach extremely high temperatures.

To prove the case, the optimal sequence was compared with the initial set of experiments using sequences of double pulses separated by 10 and 22 ps with the same total energy, and the recorded yield was comparable. Since the linear free-electron absorption dominates the energy deposition in the liquid phase, the particular shape of the second pulse no longer plays a significant role, as long as the pulse is shorter than thermal conduction and the liquid phase is already present, and this makes available a large selection of optimal solutions. The amount of energy deposited in the liquid layer is then simply given by $\int_{\tau}^{\infty} [1 - R(t)] I(t) dt$,

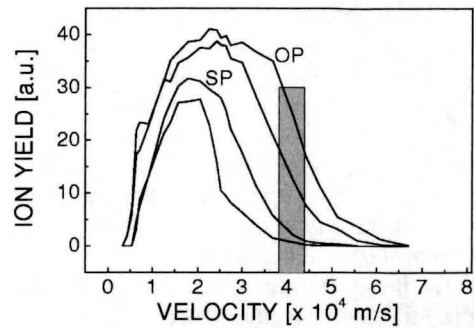


Fig. 7 Si^+ ion velocity distributions for different signal target functions, showing the tunability of the kinetic properties of the ions. The fastest distribution corresponds to irradiation with the optimal pulse. The velocity window used in optimization is marked.

where τ denotes the onset of the phase transition, and $R(t)$ is the transient reflectivity. The velocity distribution corresponding to the optimal irradiation is presented in Fig. 7 as the fastest distribution. The broad velocity envelope suggests the presence of several stream velocity components corresponding to different stages of removal. Since the emission process may require a finite amount of time, with variable conditions at the vacuum-solid interface, the distribution of the ejected particles may include different drift velocities and translational temperatures.⁴⁶ Similar fast velocity features can be induced by a single short pulse with an energy density superior to 1.6 J/cm^2 , i.e., twice as much as used for the optimization experiments. The possibility of defining the fitness function according to specific target signals enables one to access also the gray levels between the zero level and the maximum ion value by redistributing the energy between the two main features of the optimal pulse. Optimization of different velocity windows for the ions opens up the possibility to generate ion beams with tunable kinetic properties on the expense of the absolute number of ions produced. Figure 7 shows several velocity distributions covering a large spectrum of accessible energies for the emitted ions when temporally selective excitation is used, enabling accurate control of the degree of superheating.

To confirm the real-time development of the laser-triggered processes we performed a time-resolved experiment detecting the reflected part of a p -polarized weak probe pulse in a cross-polarized, collinear pump-probe setup after previous excitation with short singular pulses with different amounts of energy. Monitoring the transient reflectivity enables the possibility to follow in time the energy redistribution and fast electronic and structural modifications. The irradiation geometry was kept similar to the optimization experiment. The 24-deg laser incidence enables good discrimination between the electronic and structural changes. No particular care was taken to match the size of the probe with the region of uniform excitation, the recorded signal corresponding to the spatially averaged reflectivity. Although the reflectivities alone cannot provide the complete picture, corroborated with previously reported imaging experiments^{35,37} and time-resolved x-ray detection,^{32,33} one can obtain a satisfactory prognosis. At low input energies, close to the melting threshold and equal to the energy content of the first peak in the optimal se-

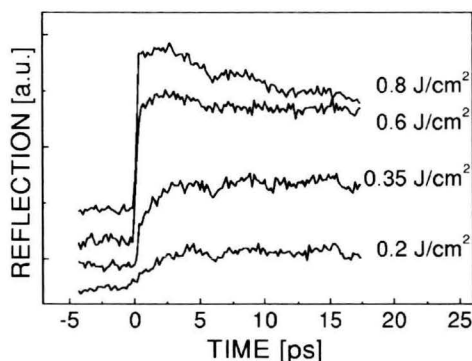


Fig. 8 Time-resolved reflectivity of the excited silicon surface at different irradiation doses as a probe for laser-induced electronic and structural modifications. The short pump pulse is centered at $t=0$.

quence, a slow increase of the reflectivity is observed, which levels out after more than 5 ps. If we increase the pump energy, the situation gradually changes, culminating with the appearance of the fast, subpicosecond nonthermal transition to the disordered phase (Fig. 8). Replacing the initially short pump pulse with the optimal excitation sequence indicates a slow increase of the reflectivity (not shown here), peaking 8 ps after the initial spike, and confirming the scenario presented for the temporal development of the energy coupling.⁴²

The evolution of the thermodynamical states of the material under the optimal irradiation sequence was followed⁴² using the 1-D drift-diffusion continuum approach developed in Ref. 29. The theoretical method follows the electronic and thermal transport in excited silicon samples by solving the continuity equation and accounting for the laser energy transfer to the electrons and, subsequently, to the lattice, followed by the nucleation of the liquid phase.⁴⁷ On these timescales, normal equilibrium boiling, which involves bubble formation and diffusion, is severely limited and circumstances are created so that strong superheating of the liquid can be achieved. After nucleating the liquid phase by the initial pulse, under conditions of stress confinement, the heating rate becomes so intense that the liquid layer is pushed into a supercritical fluid state. Complementing the continuum model with the molecular dynamic simulation results of Perez and Lewis⁴⁸ and Lorazo et al.,⁴⁹ a physically relevant picture of the successive events emerges. The unstable fluid exposed to the second, long pulse decomposes into a collection of gas and clusters as a result of the nearly adiabatic expansion above or across the spinodal.

4 Conclusions

We presented experimental results describing the influence of temporal shaping of ultrafast laser pulses on laser-irradiated materials at input energies above the threshold for material removal. Suitable temporally shaped pulses enable us to exploit ultrafast structural transformations that lead to an improvement of the energetic coupling. A brief review of possible applications for processing of dielectric materials with relatively strong electron-phonon coupling was presented, showing that the energy flow and the material response can be guided to improve processing results. Illustrative situations for CaF_2 and a-SiO_2 were described.

The primary absorption process was illustrated by time-resolved monitoring of the self-action (transmission and reflection) of an ultrafast laser pulse above the material damage threshold. Further insight into the mechanisms of material removal is gained from TOF mass spectrometry on neutral and charged particles emitted from dielectric materials. Nonthermal and thermal mechanisms were advocated based on the dynamic response and the particular shape of the kinetic distributions of the emitted particles. Also, examples were given to illustrate the possibility of manipulating the properties of ion beams generated during laser ablation of Si wafers. We demonstrated that adaptive evolutionary optimization schemes and pulse temporal tailoring can have an extended range of action, enabling applications that could largely benefit from the synergies between laser action and the material characteristic response. In this particular respect, our results show that it is possible to adaptively optimize the kinetic properties of ions emitted from laser-irradiated semiconductor samples using excitation sequences synchronized with the phase transformation characteristic times, exploiting transitions to supercritical fluid states. Corroborating different experimental approaches, from TOF mass spectrometry to time-resolved reflectivity measurements, theoretical calculations, and previously published data on molecular dynamic simulations of laser-excited materials, we described a conceivable thermodynamic evolution path for the system around the critical point. This paper demonstrates the additional advantages of utilizing temporally tailored ultrafast laser pulses, laying the basis for the possibility of generating ion beams with specific energetic properties whenever optimally designed excitation pulses are used for irradiation.

Acknowledgments

The European Union (EU) access to research infrastructure programs under the Contracts HPRI-CT-1999-00084 and HPRI-CT-2001-00139 and the Wissenschaftlich-Technologischen Zusammenarbeit (WTZ) project RUS01/224 are gratefully acknowledged.

References

1. E. N. Glezer and E. Mazur, "Ultrafast-laser driven micro-explosions in transparent materials," *Appl. Phys. Lett.* **71**(7), 882–884 (1997).
2. F. Korte, S. Nolte, B. N. Chichkov, T. Bauer, G. Kamlage, T. Wagner, C. Fallnich, and H. Welling, "Far-field and near-field material processing with femtosecond laser pulses," *Appl. Phys. A: Mater. Sci. Process.* **69**(Suppl. S), S7–S11 (1999).
3. X. Liu, D. Du, and G. Mourou, "Laser ablation and micromachining with ultrashort laser pulses," *IEEE J. Quantum Electron.* **33**(10), 1706–1716 (1997).
4. M. Lezner, J. Krüger, S. Sartania, Z. Cheng, Ch. Spielmann, G. Mourou, W. Kautek, and F. Krausz, "Femtosecond optical breakdown in dielectrics," *Phys. Rev. Lett.* **80**(18), 4076–4079 (1998).
5. F. Korte, S. Adams, A. Egbert, C. Fallnich, and A. Ostendorf, "Subdiffraction limited structuring of solid targets with femtosecond laser pulses," *Opt. Express* **7**(2), 41–49 (2000).
6. B. C. Stuart, M. D. Feit, A. M. Rubenchik, B. W. Shore, and M. D. Perry, "Laser-induced damage in dielectrics with nanosecond to subpicosecond pulses," *Phys. Rev. Lett.* **74**(12), 2248–2251 (1995).
7. A.-C. Tien, S. Backus, H. C. Kapteyn, M. M. Murnane, and G. Mourou, "Short-pulse laser damage in transparent materials as a function of pulse duration," *Phys. Rev. Lett.* **82**(19), 3883–3886 (1999).
8. D. Ashkenasi, H. Varel, A. Rosenfeld, F. Noack, and E. E. B. Campbell, "Pulsewidth influence on laser structuring of dielectrics," *Nucl. Instrum. Methods Phys. Res. B* **122**(3), 359–363 (1997).

9. H. Varel, D. Ashkenasi, A. Rosenfeld, R. Herrmann, F. Noack, and E. E. B. Campbell, "Laser-induced damage in SiO₂ and CaF₂ with picosecond and femtosecond laser pulses," *Appl. Phys. A: Mater. Sci. Process.* **62**(3), 293–294 (1996).
10. R. Stoian, M. Boyle, A. Thoss, A. Rosenfeld, G. Korn, E. E. B. Campbell, and I. V. Hertel, "Laser ablation of dielectrics with temporally shaped femtosecond pulses," *Appl. Phys. Lett.* **80**(3), 353–355 (2002).
11. A. M. Weiner, "Femtosecond pulse shaping using spatial light modulators," *Rev. Sci. Instrum.* **71**(5), 1929–1960 (2000).
12. J. P. Heritage, R. N. Thurston, W. J. Tomlinson, A. M. Weiner, and R. H. Stollen, "Spectral windowing of frequency-modulated optical pulses in a grating compressor," *Appl. Phys. Lett.* **47**(2), 87–89 (1985).
13. R. S. Judson and H. Rabitz, "Teaching lasers to control molecules," *Phys. Rev. Lett.* **68**(10), 1500–1503 (1992).
14. D. Meshulach and Y. Silberberg, "Coherent quantum control of two-photon transitions by a femtosecond laser pulse," *Nature (London)* **396**(6708), 239–242 (1998).
15. T. C. Weinacht, R. Bartels, S. Backus, P. H. Bucksbaum, B. Pearson, J. M. Geremia, H. Rabitz, H. C. Kapteyn, and M. M. Murnane, "Coherent learning control of vibrational motion in room temperature molecular gases," *Chem. Phys. Lett.* **344**(3–4), 333–338 (2001).
16. T. Feurer, J. C. Vaughan, and K. A. Nelson, "Spatiotemporal coherent control of lattice vibrational waves," *Science* **299**(5605), 374–377 (2003).
17. A. Assion, T. Baumert, M. Bergt, T. Brixner, B. Kiefer, V. Seyfried, M. Strehle, and G. Gerber, "Control of chemical reactions by feedback-optimized phase-shaped femtosecond laser pulses," *Science* **282**(5390), 919–922 (1998).
18. R. Bartels, S. Backus, E. Zeek, L. Misoguti, G. Vdovin, I. P. Christov, M. M. Murnane, and H. C. Kapteyn, "Shaped-pulse optimization of coherent emission of high-harmonic soft x-rays," *Nature (London)* **406**(6792), 164–166 (2000).
19. J. Kunde, B. Baumann, S. Arlt, F. Morier-Genoud, U. Siegner, and U. Keller, "Optimization of adaptive feedback control for ultrafast semiconductor spectroscopy," *J. Opt. Soc. Am. B* **18**(16), 872–881 (2001).
20. M. Spyridaki, E. Koudoumas, P. Tzanetakakis, C. Fotakis, R. Stoian, A. Rosenfeld, and I. V. Hertel, "Temporal pulse manipulation and ion generation in ultrafast laser ablation of silicon," *Appl. Phys. Lett.* **83**(7), 1474–1476 (2003).
21. H. Varel, M. Wahmer, A. Rosenfeld, D. Ashkenasi, and E. E. B. Campbell, "Femtosecond laser ablation of sapphire: time-of-flight analysis of ablation plume," *Appl. Surf. Sci.* **127–129**, 128–133 (1998).
22. R. Stoian, H. Varel, A. Rosenfeld, D. Ashkenasi, R. Kelly, and E. E. B. Campbell, "Ion time-of-flight analysis of ultrashort pulsed laser-induced processing of Al₂O₃," *Appl. Surf. Sci.* **165**(1), 44–55 (2000).
23. J. Siegel, K. Etrich, E. Welsch, and E. Matthias, "UV-laser ablation of ductile and brittle metal films," *Appl. Phys. A: Solids Surf.* **64**(2), 213–218 (1997).
24. S. Guizard, P. D. Oliveira, P. Daguzan, P. Martin, P. Meynadier, and G. Petite, "Time-resolved studies of carriers dynamics in wide band gap materials," *Nucl. Instrum. Methods Phys. Res. B* **116**(1–4), 43–48 (1996).
25. F. Quere, S. Guizard, P. Martin, G. Petite, O. Gobert, P. Meynadier, and M. Perdrix, "Ultrafast carrier dynamics in laser-excited materials: subpicosecond optical studies," *Appl. Phys. B: Lasers Opt.* **68**(3), 459–463 (1999).
26. M. Li, S. Menon, J. P. Nibarger, and G. N. Gibson, "Ultrafast electron dynamics in femtosecond optical breakdown of dielectrics," *Phys. Rev. Lett.* **82**(11), 2394–2397 (1999).
27. R. Lindner, M. Reichling, R. T. Williams, and E. Matthias, "Femtosecond laser pulse excitation of electrons and excitons in CaF₂ and SrF₂," *J. Phys.: Condens. Matter* **13**(10), 2339–2346 (2001).
28. R. Stoian, M. Boyle, A. Thoss, A. Rosenfeld, G. Korn, and I. V. Hertel, "Dynamic temporal pulse shaping in advanced ultrafast laser material processing," *Appl. Phys. A: Solids Surf.* **77**(2), 265–269 (2003).
29. N. M. Bulgakova, R. Stoian, A. Rosenfeld, I. V. Hertel, and E. E. B. Campbell, "Electronic transport and consequences for material removal in ultrafast pulsed laser ablation of materials," *Phys. Rev. B* **69**(5), 054102 (2004).
30. R. Stoian, A. Rosenfeld, D. Ashkenasi, I. V. Hertel, N. M. Bulgakova, and E. E. B. Campbell, "Surface charging and impulsive ion ejection during ultrashort pulsed laser ablation," *Phys. Rev. Lett.* **88**(9), 097603 (2002).
31. R. Stoian, D. Ashkenasi, A. Rosenfeld, and E. E. B. Campbell, "Coulomb explosion in ultrashort pulsed laser ablation of Al₂O₃," *Phys. Rev. B* **62**(19), 13167–13173 (2000).
32. C. W. Siders, A. Cavalleri, K. Sokolowski-Tinten, C. Toth, T. Guo, M. Kammler, M. H. von Hoegen, K. R. Wilson, D. von der Linde, and C. P. J. Barty, "Detection of nonthermal melting by ultrafast x-ray diffraction," *Science* **286**(5443), 1340–1342 (1999).
33. A. Rousse, C. Rischel, S. Fourmaux, I. Uschmann, S. Sebban, G. Grillon, P. Balcou, E. Foster, J. P. Geindre, P. Audebert, J. C. Gauthier, and D. Hulin, "Non-thermal melting in semiconductors measured at femtosecond resolution," *Nature (London)* **410**(6824), 65–68 (2001).
34. J. P. Callan, A. M.-T. Kim, C. A. D. Roeser, and E. Mazur, "Universal dynamics during and after ultrafast laser-induced semiconductor-to-metal transitions," *Phys. Rev. B* **64**(7), 073201 (2001).
35. C. V. Shank, R. Yen, and C. Hirlmann, "Femtosecond-time-resolved surface structural dynamics of optically excited silicon," *Phys. Rev. Lett.* **51**(10), 900–902 (1983).
36. P. Stampfli and K. H. Bennemann, "Theory for the time dependence of the laser-induced instability of the diamond structure of Si and GaAs," *J. Phys.: Condens. Matter* **5**(Suppl. 33A), A173–A174 (1993).
37. K. Sokolowski-Tinten, J. Bialkowski, A. Cavalleri, D. von der Linde, A. Oparin, J. Meyer-ter-Vehn, and S. I. Anisimov, "Transient states of matter during short pulse laser ablation," *Phys. Rev. Lett.* **81**(1), 224–227 (1998).
38. K. Sokolowski-Tinten, J. Solis, J. Bialkowski, J. Siegel, C. N. Afonso, and D. von der Linde, "Dynamics of ultrafast phase changes in amorphous GeSb films," *Phys. Rev. Lett.* **81**(17), 3679–3682 (1998).
39. K. Sokolowski-Tinten and D. von der Linde, "Generation of dense electron-hole plasmas in silicon," *Phys. Rev. B* **61**(4), 2643–2650 (2000).
40. S. Amoruso, X. Wang, C. Altucci, C. de Lisio, M. Armenante, R. Bruzese, and R. Veletta, "Thermal and nonthermal ion emission during high-fluence femtosecond laser ablation of metallic targets," *Appl. Phys. Lett.* **77**(23), 3728–3730 (2000).
41. T. Y. Choi, D. J. Hwang, and C. P. Grigoropoulos, "Femtosecond laser induced ablation of crystalline silicon upon double beam irradiation," *Appl. Surf. Sci.* **197–198**, 720–725 (2002).
42. R. Stoian, A. Mermillod-Blondin, A. Rosenfeld, I. V. Hertel, M. Spyridaki, E. Koudoumas, P. Tzanetakakis, C. Fotakis, and N. M. Bulgakova, "Adaptive optimization of ultrafast laser generated low-energy ion beams from silicon targets," (*submitted for publication*).
43. A. Bartelt, "Control of wave packet dynamics in small alkali clusters with optimally shaped femtosecond pulses," PhD Thesis, Freie Universität Berlin (2002).
44. A. Hache, Y. Kostoulas, R. Atanasov, J. L. P. Hughes, J. E. Sipe, and H. M. van Driel, "Observation of coherently controlled photocurrent in unbiased, bulk GaAs," *Phys. Rev. Lett.* **78**(2), 306–309 (1997).
45. G. E. Jellison and D. H. Lowndes, "Measurements of the optical properties of liquid silicon and germanium using nanosecond time-resolved ellipsometry," *Appl. Phys. Lett.* **51**(5), 352–354 (1987).
46. L. V. Zhigilei and B. J. Garrison, "Velocity distributions of molecules ejected in laser ablation," *Appl. Phys. Lett.* **71**(4), 551–553 (1997).
47. B. Rethfeld, K. Sokolowski-Tinten, D. von der Linde, and S. Anisimov, "Ultrafast thermal melting of laser-excited solids by homogeneous nucleation," *Phys. Rev. B* **65**(9), 092103 (2002).
48. D. Perez and L. J. Lewis, "Molecular-dynamics study of ablation of solids under femtosecond laser pulses," *Phys. Rev. B* **67**(18), 184102 (2003).
49. P. Lorazo, L. J. Lewis, and M. Meunier, "Short-pulse laser ablation of solids: From phase explosion to fragmentation," *Phys. Rev. Lett.* **91**(22), 225502 (2003).



Razvan Stoian graduated in 1995 from the Bucharest University, Romania, and received his PhD degree from the Free University, Berlin, in 2000. Since 1997, he has been a member of the Ultrafast Laser Material-Processing Group at the Max-Born Institute, Berlin, Germany.



Alexandre Mermillod-Blondin graduated in 2003 from the University Jean Monnet, Saint-Etienne, France, where he is currently a PhD student in the Laboratoire Traitement du Signal et de l'Image, and also at the Max Born Institute, Berlin, Germany.



Sebastian W. Winkler graduated in 2003 from the Technischen Universität Berlin, Germany. He is currently a research scholar at the University of Georgia, Athens.

Arkadi Rosenfeld Biography and photograph not available.

Ingolf V. Hertel Biography and photograph not available.

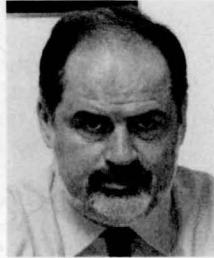


Maria Spyridaki studied physics at the University of Crete, where she received a BSc degree in physics and an MSc degree in microelectronics-optoelectronics from the Physics Department. She is currently a PhD student with the University of Crete performing research on laser-material interactions at the Institute of Electronic Structure and Laser (IESL-FORTH).



Emmanuel Koudoumas is an associate professor of electrical engineering with the Technological Educational Institute of Crete, Greece. He also holds a research position with the Institute of Electronic Structure and Lasers of the Foundation of Research and Technology-Hellas. He graduated from the Physics Department of University of Athens and received his PhD degree in applied physics from the University of Patras, Greece, in 1991. His main research interests include high-intensity short-pulse laser-matter interactions and the nonlinear optical response of materials.

Panos Tzanetakis received his PhD degree from the University of Grenoble and was with the Materials Research Laboratory (MRL) of the University of Illinois at Urbana-Champaign. He is now an associate professor of physics at the University of Crete and also holds a research position at the Foundation for Research and Technology-Hellas (FORTH). His research interests include thin semiconductor films, photovoltaics, laser-materials interaction, and scanning probe nanoscale techniques.



Costas Fotakis directs the Institute of Electronic Structure and Laser (IESL) at FORTH (Foundation for Research and Technology-Hellas) and is a professor of physics with the University of Crete. He also directs the Ultraviolet Laser Facility operating at FORTH. His research interests include laser spectroscopy, molecular photophysics, laser interactions with materials, and related applications for material processing and analysis.



Igor M. Burakov studied physics at the Novosibirsk State University, Russia, and received his BSc degree in physics in 2000 and his MSc degree in physics of nonequilibrium processes in 2002. He is currently a PhD student at the Institute of Thermophysics SB RAS, Novosibirsk, Russia. His research interests are related to numerical modeling of femtosecond laser interaction with solids.



Nadezhda M. Bulgakova studied physics at the Novosibirsk State University, Russia. After graduation, she joined the Institute of Thermophysics (Siberian Branch of Russian Academy of Sciences) where she received her PhD degree in 1985 and her DrSc degree in 2002. Her research interests include various aspects of laser-matter interaction and classical gas dynamics and hydrodynamics.